

## AERODYNAMIC CHARACTERISTICS OF TWO-, THREE- AND FOUR-BLADED STATIONARY SAVONIUS ROTORS

M. Quamrul Islam\* M. Sharif-ul-Hasan\*\* F.H. Chowdhury\*\*

### ABSTRACT

*Static torque and drag coefficients of a stationary Savonius rotor with two, three and four blades have been investigated by measuring the pressure distribution on the blade surfaces for different rotor angles. Experiments have been performed at a Reynolds no.  $1.8 \times 10^5$  with rotors having semi-circular blade profile with an overlap ratio of 0.2. Results indicate that static torque coefficients vary considerably with the rotor angle. These results were used to compare the performance of two-, three- and four-bladed Savonius rotors under dynamic conditions.*

**Keywords:** *Savonius rotor, Semi-circular blade profile, Static torque coefficients, Dynamic condition.*

### Nomenclature

$C_q$	Torque coefficient of a single blade
$C_Q$	Total Torque coefficient of the rotor
$C_n$	Normal force coefficient
$C_t$	Tangential force coefficient
$C_p$	Power coefficient
$d$	Diameter of blade
$F_n$	Normal force
$F_t$	Tangential force
$R$	Radius of rotor
$S$	Overlap ratio
$U_o$	Free stream velocity
$\lambda$	Tip speed ratio ( $R \Omega / U_o$ )
$\Omega$	Speed of rotor

---

\* Professor, Bangladesh University of Engineering & Technology (BUET), Dhaka, Bangladesh.

\*\* Lecturer, Bangladesh University of Engineering & Technology (BUET), Dhaka, Bangladesh.

## 1. INTRODUCTION

The Savonius rotor has been a subject of interest since the 1930's and has been studied extensively. It is a vertical axis wind turbine and has a lower efficiency as compared to other vertical axis wind turbines, such as Darrieus rotor. Nevertheless, it is used as an alternative to wind power extraction because of its simple design and good starting torque at low wind speeds [1,5,10,14]. Rigorous studies on the performance characteristics of the Savonius rotor are found in the literatures and these enable the identification of an optimum geometrical configuration for practical design [2,4,6,9,11]. However, only a few studies are reported in the literatures, which give information regarding the total aerodynamic load on the structure and mechanism of rotation of the rotor. This paper attempts an experimental study on the aerodynamic load on a stationary Savonius rotor with different multiple number of blades.

## 2. EXPERIMENTAL SETUP AND PROCEDURE

The objectives of the investigation of wind loading on the semi-cylindrical bladed Savonius rotors have been realized essentially with the help of a subsonic wind tunnel, experimental setup of the Savonius rotor with 2, 3 and 4 blades and an inclined manometer bank. The schematic diagram of wind tunnel is shown in Figure 1.

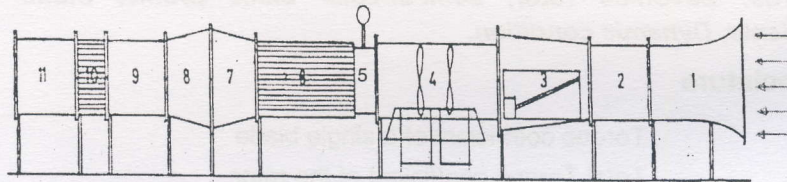


Figure 1: Schematic Diagram of Wind Tunnel

- |                                    |                               |
|------------------------------------|-------------------------------|
| 1. Converging Mouth Entry          | 7. Diverging Section          |
| 2. Perspex Section                 | 8. Converging Section         |
| 3. Rectangular Diverging Section   | 9. Rectangular Section        |
| 4. Fan Section                     | 10. Flow Straightener Section |
| 5. Butterfly Section               | 11. Rectangular Exit Section  |
| 6. Silencer with Honeycomb Section |                               |

### 2.1 The Wind Tunnel

The open circuit subsonic wind tunnel is 6.55 m long with a test section of 490 x 490 mm cross-section. The successive sections of the wind tunnel comprise of converging mouth entry, perspex section, rectangular section, fan section (two rotary axial flow fans), butterfly section, silencer with honey comb section, an eddy breaker, diverging section, converging section, 610 mm long rectangular section, 305 mm long flow straightener section and 610 mm long rectangular exit



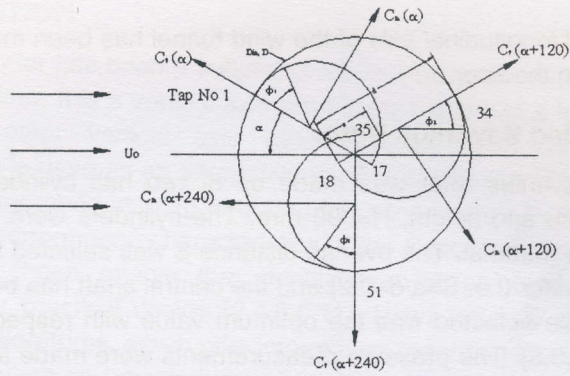


Figure 3: Forces Acting on Three-Bladed Savonius Rotor.

## 2.4 The Four-Bladed Savonius Rotor

The four-bladed Savonius rotor (Fig.4) was made up of four half cylinders (blade) of diameter,  $d=125$  mm and height,  $H=300$  mm. The cylinders were made of PVC material. The overlap ratio  $S$  was selected to be one-fifth of the cylinder diameter (i.e.  $S = a/d = 0.2$ ) and the central shaft had been removed. The overlap distance selected was the optimum value with respect to the wind power extraction. The whole rotor was fixed on an iron frame by using two side shafts and two ball bearings. The pressure measurements were made at 17 pressure tapplings on each blade. The tapplings were made with copper tubes of 1.5 mm outer diameter and 10 mm length which were pressed fitted to the tapping holes. The tapplings were located at the mid-plane on one side of each blade, so that pressure distribution at every  $10^\circ$  on the blade surface could be measured. The pressure tapplings were connected to an inclined manometer bank (manometric fluid being water with an accuracy of  $\pm 0.1$  mm of water column) through 2 mm tubes. The pressures were measured at every  $10^\circ$  interval of rotor angle.

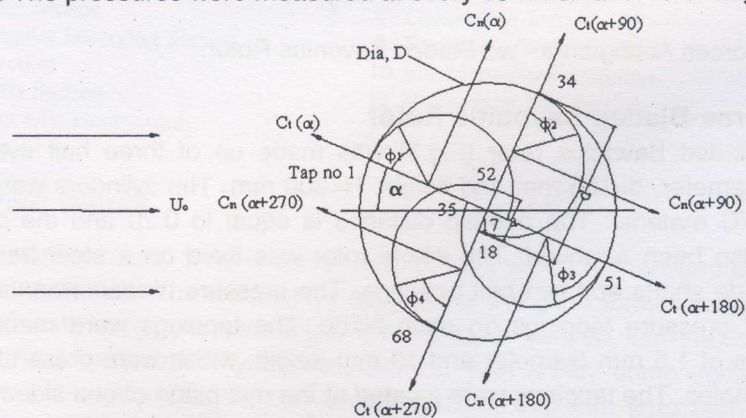


Figure 4: Forces Acting on Four-Bladed Savonius Rotor.

## 2.5 Aerodynamic Characteristics Calculation

The flow pattern produced by the rotor blades is characterized by complicated flow phenomenon such as high turbulence, unsteadiness and flow separation [1,6,11,14]. The combined of these flow features in turn produces pressure differences between the front and back surfaces of the blades. These pressure differences result in the calculation of aerodynamic forces from numerical integrations.

The pressure coefficient can be defined by,

$$C_p = \frac{p - p_o}{\frac{1}{2} \rho U_o^2} \quad (1)$$

Where,  $p - p_o$  = Difference between measured pressure and atmospheric pressure.

$\rho$  = Density of air.

$U_o$  = Free stream velocity.

For Savonius rotor at a particular rotor angle,  $\alpha$  the rotor blades experiences forces (per unit span length) due to the pressure difference between the concave surface and convex surface and these forces can be resolved into two components  $F_n$  and  $F_t$ . Since the blade surfaces are circular,  $F_n$  and  $F_t$  pass through the center of the semicircle. The drag coefficient in normal and tangential directions can be written as follows:

$$C_n = \frac{F_n}{\frac{1}{2} \rho U_o^2 d}, \quad C_t = \frac{F_t}{\frac{1}{2} \rho U_o^2 d} \quad (2)$$

To obtain the drag coefficients in the normal and tangential direction of the chord, the value of  $F_n$  and  $F_t$  are obtained by integrating the pressure for a blade as follows:

$$F_n = \int_0^\pi \Delta p \frac{d}{2} \cos \phi d\phi = \sum_{i=1}^{17} \Delta p_i \frac{d}{2} \cos \phi_i \Delta \phi_i \quad (3)$$

$$\text{and similarly, } F_t = \sum_{i=1}^{17} \Delta p_i \frac{d}{2} \sin \phi_i \Delta \phi_i \quad (4)$$

Where  $\Delta p_i$  is the difference in pressure on the concave and convex surfaces at a particular pressure tapping, i. This  $\Delta p_i$  is multiplied by the differential area  $\frac{d}{2} \cdot 1 \cdot d\phi$ , considering unit height of the blade to obtain the value of differential tangential and normal forces. Then numerical integration is carried out for the whole diameter of each blade considering the limit 0 to  $\pi$  for obtaining the value of  $F_t$  and  $F_n$ . The force  $F_n$  is responsible for producing a torque on the shaft of the rotor and this torque coefficient for a single blade at a particular rotor angle can be written as:

$$C_q(\alpha) = C_n(\alpha) \frac{(1-S)}{(2-S)^2} \quad (5)$$

The total static torque coefficient produced on the rotor shaft for a two-bladed Savonius rotor can be expressed as follows:

$$C_Q(\alpha) = [C_n(\alpha) + C_n(\alpha + 180^\circ)] \frac{(1-S)}{(2-S)^2} \quad (6)$$

Where,  $C_n(\alpha)$  and  $C_n(\alpha + 180^\circ)$  refer to the drag coefficients of the advancing and returning blade respectively at rotor angle,  $\alpha$ .

The total static torque coefficient produced on the rotor shaft for a three-bladed Savonius rotor can be expressed as follows:

$$C_Q(\alpha) = [C_n(\alpha) + C_n(\alpha + 120^\circ) + C_n(\alpha + 240^\circ)] \frac{(1-S)}{(2-S)^2} \quad (7)$$

Where,  $C_n(\alpha)$ ,  $C_n(\alpha + 120^\circ)$  and  $C_n(\alpha + 240^\circ)$  refer to the drag coefficients of the first, second and third blade respectively at rotor angle,  $\alpha$ .

The total static torque coefficient produced on the rotor shaft for a four-bladed Savonius rotor can be expressed as follows:

$$C_Q(\alpha) = [C_n(\alpha) + C_n(\alpha + 90^\circ) + C_n(\alpha + 180^\circ) + C_n(\alpha + 270^\circ)] \frac{(1-S)}{(2-S)^2} \quad (8)$$

Where,  $C_n(\alpha)$ ,  $C_n(\alpha + 90^\circ)$ ,  $C_n(\alpha + 180^\circ)$  and  $C_n(\alpha + 180^\circ)$  refer to the drag coefficients of the first, second, third and fourth blade respectively at rotor angle,  $\alpha$ .

### 3. RESULTS AND DISCUSSION

Normal drag coefficient,  $C_n$  of an individual blade of two bladed Savonius rotor, four bladed Savonius rotor and three bladed Savonius rotor [3] is shown in Fig.5

for different rotor angles. For the flow over the four bladed system, considering a single blade, the normal drag coefficient  $C_n(\alpha)$  increases with the increase of rotor angle from  $\alpha=0^\circ$  to  $20^\circ$ . From this point the drag coefficient  $C_n$  decreases with the increase of rotor angle  $\alpha$  up to  $90^\circ$ . Between  $\alpha=0^\circ$  to  $90^\circ$ , the drag coefficient  $C_n(\alpha)$  is positive for rotor angle  $0^\circ$  to  $60^\circ$  and reaches its maximum value at  $\alpha=20^\circ$ . At  $\alpha=100^\circ$ , the value of  $C_n$  increases after which it remains constant till  $\alpha=150^\circ$ . Between  $\alpha=150^\circ$  to  $160^\circ$ , the value of  $C_n$  drops slightly and then remains constant till  $\alpha=180^\circ$ . The  $C_n$  decreases between  $\alpha=180^\circ$  to  $210^\circ$ . Again from  $\alpha=210^\circ$ ,  $C_n$  increases sharply up to  $250^\circ$  and from  $\alpha=260^\circ$  to  $320^\circ$   $C_n$  falls sharply and become negative. Between  $\alpha=220^\circ$  to  $300^\circ$ , the drag coefficient  $C_n$  is responsible for maximum torque production. For the flow over the three bladed Savonius rotor [3], for a single blade, normal drag coefficient  $C_n(\alpha)$  increases with the increase of rotor angle from  $\alpha=0^\circ$  to  $60^\circ$  and then decreases with the increase of the rotor angle,  $\alpha$  up to  $120^\circ$ . It remains constant from  $\alpha=120^\circ$  to  $220^\circ$ . From  $\alpha=230^\circ$ , drag coefficient increases till  $\alpha=260^\circ$  and decreases from  $\alpha=270^\circ$  to  $340^\circ$ . Again at  $\alpha=340^\circ$ , drag coefficient  $C_n$  increases and becomes zero at  $\alpha=350^\circ$ . For the flow over the two bladed Savonius rotor, for a single blade, normal drag Coefficient  $C_n(\alpha)$  are positive from  $\alpha=0^\circ$  to  $160^\circ$  and then become negative for  $170^\circ$ , then again become positive from  $180^\circ$  to  $260^\circ$  and negative upto  $360^\circ$ . The maximum normal drag coefficient for this two bladed Savonius rotor is at  $60^\circ$  and minimum at  $300^\circ$ .

The tangential drag coefficient  $C_t$ , with individual blade effect for two bladed system, three bladed system and four bladed system is shown in Fig.6 for different rotor angles. In case of four bladed system considering a single blade, the tangential drag coefficient  $C_t$  increases with the increase of rotor angle from  $\alpha=0^\circ$  to  $20^\circ$ . From this point,  $C_t$  decreases up to  $\alpha=130^\circ$ . From  $\alpha=130^\circ$  to  $\alpha=200^\circ$ , the value of  $C_t$  is constant and nearly equal to zero. From  $\alpha=210^\circ$  tangential drag coefficient increases till  $\alpha=220^\circ$ . The drag coefficient decreases from  $\alpha=220^\circ$  to  $\alpha=310^\circ$  and again it increases from  $\alpha=320^\circ$  to  $360^\circ$ . The negative thrust is produced from  $\alpha=270^\circ$  to  $\alpha=340^\circ$ . Finally, it produces positive thrust at  $\alpha=350^\circ$ . Maximum positive thrust is available between  $0^\circ$  to  $110^\circ$  angle of rotation and maximum negative thrust is available from  $\alpha=270^\circ$  to  $340^\circ$  angle of rotation. Whereas for the three bladed system, tangential drag coefficients  $C_t$  increases with the increase of rotor angle from  $\alpha=10^\circ$  to  $60^\circ$ . Then it remains constant from  $60^\circ$  to  $110^\circ$  and at  $120^\circ$ ,  $C_t$  decreases. It remains positive from  $\alpha=130^\circ$  to  $230^\circ$ . Then it decreases from  $240^\circ$  to  $340^\circ$  and again increases up to  $\alpha=360^\circ$ . For the two bladed system, the tangential drag coefficient,  $C_t$  is initially negative for  $\alpha=0^\circ$  to  $20^\circ$  and then becomes positive and reached to the maximum tangential drag coefficient at  $40^\circ$ , then decreases to 0 tangential drag coefficient at  $60^\circ$ . Up to  $110^\circ$  of rotor angle the drag coefficient is nearly 0 and then increases from  $110^\circ$  to  $130^\circ$ . At the rotor angle  $160^\circ$ , it becomes negative and again increases upto

210° and almost remains same from 210° to 260° rotor angle. After 260° rotor angle the drag coefficient again decreases and reached to the lowest tangential drag coefficient value at 330° rotor angle and then remains negative upto 360°. The torque coefficient on a single blade is shown in Fig.7 for four bladed rotor system, three bladed rotor and two bladed rotor system. There is a linear relation between the normal drag coefficient,  $C_n$  and the torque coefficient,  $C_q$  for single blade [Equation 5]. So, the torque coefficient curve shows exactly same nature as the normal drag coefficient of individual blade effect.

The total torque coefficient,  $C_Q$  for two- three- and four - bladed rotor is shown in the Fig.8. From this figure, it is found that in the two bladed system, the total torque is positive upto 150° of rotor angle. Then becomes negative for the 160° and 170° rotor angle. The maximum total torque is found at 60° of rotor angle and minimum at 170° of rotor angle. In the three bladed system, the torque coefficient,  $C_Q$  rises and falls smoothly. On the other hand, the torque coefficient,  $C_Q$  rises and falls drastically in the four bladed system. By comparing the two, three and four bladed systems, the maximum total torque coefficient is found to be produced by two bladed rotor system.

#### 4. PREDICTION OF POWER COEFFICIENT

The predicted power coefficient,  $C_p$  for different tip speed ratios,  $\lambda$  are shown in Fig.9 along with the measured data of Rahman [13], Ogawa and Yoshida [12] and Islam et al [8]. The overlap ratio considered in this study is same as the rotor of Rahman, Ogawa and Yoshida, Islam et al. The predicted power coefficient matches with the result of Rahman [13] but it deviates with the result of polynomial prediction by Islam at el [8] and Ogawa and Yoshida [12] only in magnitude. This prediction method assumes a potential vortex, however, in reality the flow field around a rotating rotor is governed by time dependent shear layers, separated flows and high turbulence levels. Furthermore, the wake has not been considered in the present study. However, further research considering the complex flow behavior may give a better prediction of the performance of a Savonius rotor.

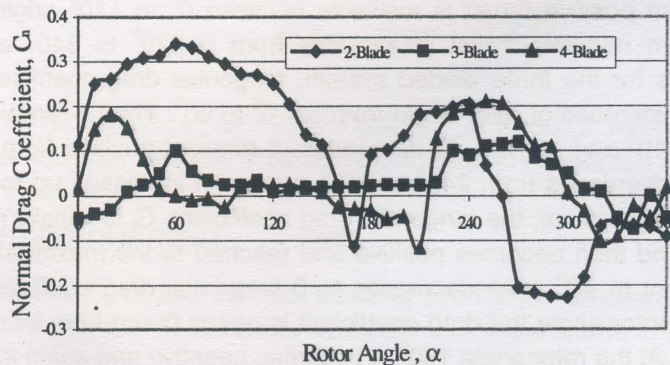


Figure 5: Normal Drag Coefficient of Individual Blade Effect

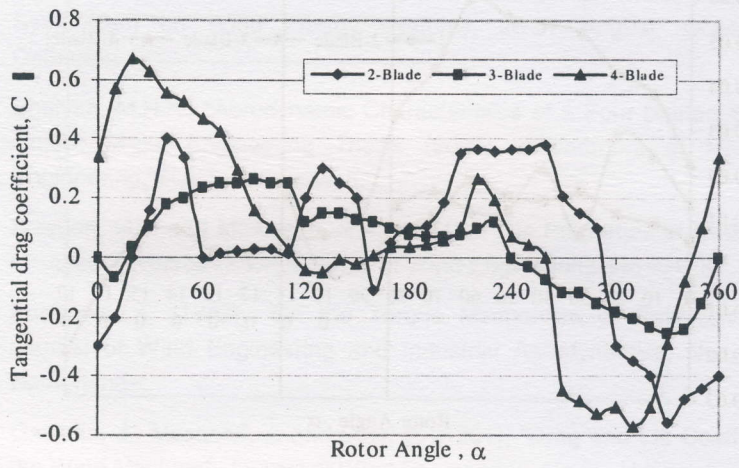


Figure 6: Tangential Drag Coefficient of Individual Blade Effect

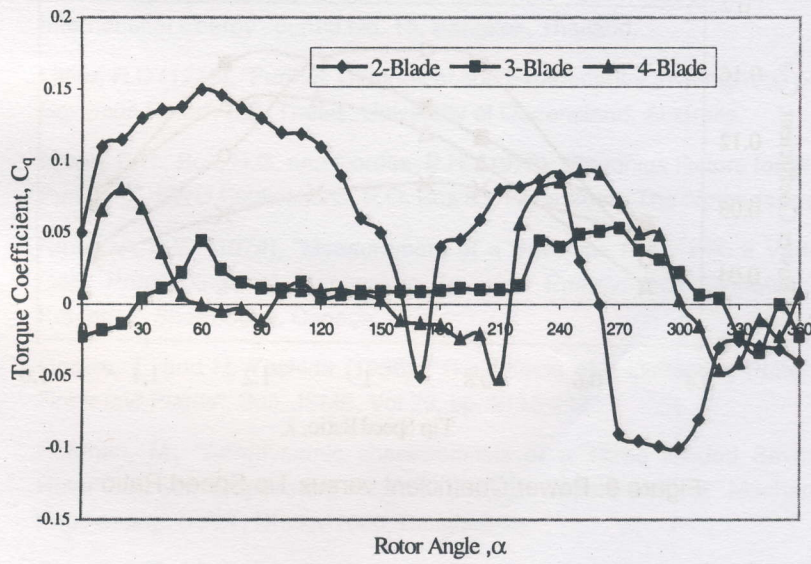


Figure 7: Torque Coefficient with Individual Blade Effect

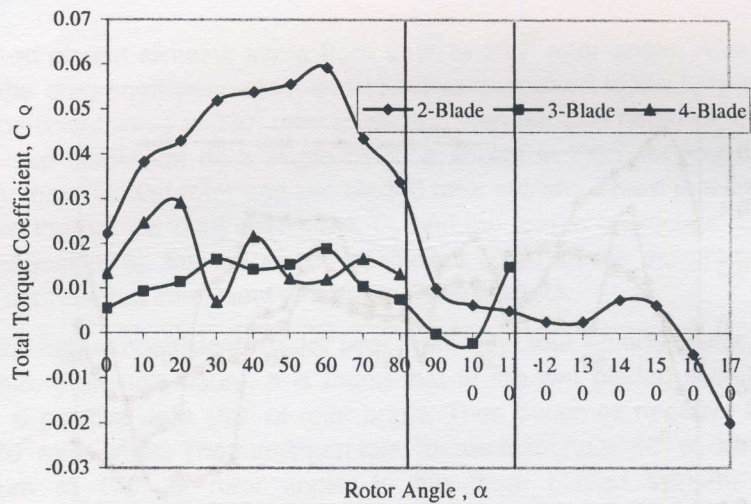


Figure 8: Total Static Torque Coefficient at Different Rotor Angles

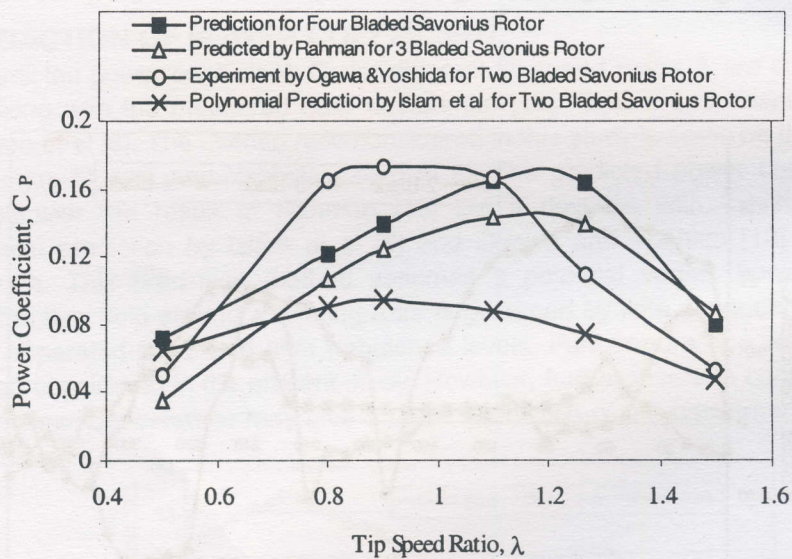


Figure 9: Power Coefficient versus Tip Speed Ratio

**REFERENCE:**

1. Aldos, T.K. and Kotb, M.A. (1991), "Aerodynamic Loads on a Stationary Savonius Rotor", JSME International Journal, Series II, No. 34, Japan.

2. Beurskens, H.J.M. (1980), "Low Speed Water Pumping Windmills: Rotor Tests and Overall Performance", Proceedings of Third International Symposium on Wind Energy Systems, 26-27 August, Copenhagen, Denmark.
3. Bhuiyan, M.H.K., "Aerodynamic Characteristics of a Four Bladed Savonius Rotor", M.Sc. Engineering Thesis (2003), Department of Mechanical Engineering, BUET, Bangladesh.
4. Bowden, G.J. and McAleese, S.A. (1984), "The Properties of Isolated and Coupled Savonius Rotor", Journal of Wind Engineering, No 8, U.K.
5. Fusisawa, n. (1992), "On the Torque Mechanism of Savonius rotors", Journal of Wind Engineering and Industrial Aerodynamics, No. 40, The Netherlands.
6. Gavadla, J., Massons, J. and Diaz, F. (1991), "Drag and Lift Coefficient of the Wind Machine", Journal of Wind Engineering, No.15, U.K.
7. Huda, M.D., Selim, M.A., Islam, A.K.M.S. and Islam, M.Q. (1992), "The Performance of an S-Shaped Savonius Rotor with a Deflecting Plate", RERIC International Energy Journal, No. 14, Bangkok, Thailand.
8. Islam, A.K.M.S., Islam M.Q., Mandal, A.C. and Razzaque, M.M. (1993), "Aerodynamic Characteristics of a Stationary Savonius Rotor", RERIC International Energy Journal No. 15, Bangkok, Thailand.
9. Littler, R.D (1975), "Further Theoretical and Experimental Investigation of the Savonius Rotor", B.E. Thesis, University of Queensland, Australia.
10. Lysen, E.H., Bos, H.G. and Cordes, E.H. (1978), "Savonius Rotors for Water Pumping", SWD Publications, P.O. Box 85, Amersfoort, The Netherlands.
11. Newman, B.G. (1974), "Measurement of a Savonius Rotor with a Variable Gap, Proceedings of Symposium on wind Energy: Achievements and Potential", Sherbrooke, Canada.
12. Ogawa, T. and H. Yoshida (1986), "The Effects of a Deflecting Plate and Rotor and Plates", Bull. JSME, Vol.29, pp. 2115-2121.
13. Rahman, M., "Aerodynamic characteristics of a Three Bladed Savonius Rotor". M.Sc. Engineering Thesis (2000), Department of Mechanical Engineering, BUET, Dhaka-1000, Bangladesh.
14. Sawada, T., Nakamura, M. and Kamada, S. (1986), "Blade Force Measurement and Flow Visualization of Savonius Rotors", Bull. JSME, Vol.29, Japan.